WIND ENERGY POTENTIAL ESTIMATION USING NEURAL NETWORK AND SVR APPROACHES

Adekunlé Akim Salami[1*] – Pierre Akuété Agbessi[1] – Seibou Boureima [2] –Ayité S. Akoda Ajavon [1]

[1]Department of Electrical Engineering, Ecole Nationale Supérieure d'Ingénieurs, Centre d'Excellence Régionale pour la Maîtrise de l'Electricité (CERME), University of Lomé, P.O. Box: 1515 Lomé, TOGO
[2]Mines, Industry and Geology school of Niamey, Niger

ARTICLE INFO

***Article history*:**
Received: 19.04.2020.
Received in revised form: 30.03.2022.
Accepted: 04.04.2022.

Keywords:
Neural Network
Support vector Regression
Multilayer perceptron
Wind energy
Weibull distribution

DOI: https://doi.org/10.30765/er.1632

Abstract:

The distribution of wind speed and the optimal assessment of wind energy potential are very important factors when selecting a suitable site for a wind power plant. In wind farm design projects for the supply of electrical energy, designers use the Weibull distribution law to analyse the characteristics and variations of wind speed in order to evaluate the wind potential. In our study we used two approaches, namely, the Multilayer Perceptron (MLP) approach and the Support Vector Machine (SVR) approach to determine a distribution law of wind speeds and to optimally evaluate the wind potential. These two approaches were compared to two well-known numerical methods which are the Justus Empirical Method (EMJ) and the Maximum Likelihood Method (MLM). The results show that the neural network approach produces a better fit of the distribution curve with an Root Mean Square Error (RMSE) of 0.00005016 at Lomé, 0.000040289 at Cotonou site and a more interesting estimate of the wind potential. After that SVR show a better result too with an RMSE of 0.0095618 at the Lomé site and 0.0053549 at the Cotonou site.

1 Introduction

The fact that fossil fuels are running out worldwide has led many researchers to focus on renewable energy sources in the last decade [1]. In addition, increasing industrialization and population growth in many countries, coupled with rising energy demand, has made renewable energy sources more popular economically and environmentally sustainable. An economic system based on fossil fuels is no longer sustainable with a significant increase in energy demand, and this tendency to promote renewable energy is one way to better reduce environmental degradation from CO2 emissions [2]. Renewable energy sources include natural energy sources such as wind, solar, geothermal, ocean and bioenergy. Among these energy sources, wind energy is of considerable importance because of its energy production potential, market value, wide range of applications and economic characteristics.

The exploitation of the wind energy plant first requires a statistical study of the site to assess its feasibility. Therefore, knowledge of the available and recoverable energy to predict the types of wind turbines to be installed is necessary. The purpose of this study is therefore to make a statistical study of wind speed measurements taken at the operating site in order to determine a distribution law, which will be necessary to evaluate the wind potential. This study is important because wind speed is considered to be a random and intermittent variable, and a simple measurement is not enough to characterize the potential of a site [3]. Various functions are used in the literature to determine the distribution law, such as the Gamma function [4-6], inverse Gamma function [7], Rayleigh distribution, lognormal, normal, Pearson type V, Kappa, Gumbel, binomial, and Weibull distribution functions [8-11]. However, the most commonly used function for modeling wind speed data is the Weibull distribution function because it gives better results compared to the other functions [12]. Elamouri and Amar Ben evaluated the wind potential at 17 sites in Tunisia using the meteorological

* Corresponding author
E-mail address: akim_salami@yahoo.fr

method and the Weibull method. The result was that the Weibull method gave better results compared to the other methods [13]. Kiss and Jánosi [14] evaluated the surface wind speed over a 44-year period with a 6-h resolution. They tested the well-known distribution functions: Rayleigh, binormal, Weibull and lognormal, and they observed that the Weibull function gives a better performance. They found that the generalized gamma distribution, which is independent of shape parameters, provides an adequate and unified solution almost everywhere.

The geographical distribution of the fitted parameters shows the possible climatological origin of the different wind speed distributions. They also found that the Weibull model can indeed characterize the wind histograms well overseas and in parts of the country. This comparison was made in Turkey and the distribution of Weibull prevailed over that of Rayleigh [15]. In Rwanda, the work of Safari et al. showed that the Weibull distribution outweighed the Rayleigh distribution in a statistical study of wind characteristics and wind potential assessment [16]. The Weibull distribution function is characterized by two parameters "k" and "c" and several numerical methods are available to express these parameters [17-18].

The best-known methods include the Moment Method (MM), Justus Empirical Method (EMJ), Maximum Likelihood Method (MLM) [19-20], Modified Maximum Likelihood Method (MMLM), Energy Structure Factor Method (EPFM), Empirical Lysen Method (EML), Graphical Method (GM) [21-22]. In order to find a better approximation of the wind speed distribution law, other approaches were used, namely: the Multilayer Perceptron (MLP) used by THIAW et al. in their work to evaluate the wind potential in Senegal [3], gave a better result than the Weibull distribution with an area ~~of~~ up to 0.997.

M. Carolin Mabel and E. Fernandez developed a model using neural network methodology that involves three input variables - wind speed, relative humidity and generation hours - and one output variable, which gives the energy output of wind farms.

This model was used to estimate the energy yield of 07 wind farms in India with a root mean square error of $7.6.10^{-3}$ [23]. A generalized feed-forward neural network (GFNN) is used by Celik and Kolhe [24] to estimate the annual wind speed distribution. It has been noted that GFNN produces a better wind speed distribution for calculating wind energy production for some wind turbine generators. Togo and Benin are a region where renewable energies are being promoted, particularly wind energy, to compensate for the energy deficit of these countries. We are interested in these countries, more specifically in the Lomé and Cotonou sites for their geographical positions and also for wind energy projects. Such is the case of the Eco Delta project which will allow the construction of the first 25.2 MW wind farm in West Africa in Togo. In our study, we will use the MLP, SVR, EMJ and MLM approaches because of their better performances to adjust the frequency histogram and to evaluate the wind potential in an optimal way [25-27]. Few studies have been done on the Lomé and Cotonou sites in relation to wind potential assessment.

The most recent one is that of Salami and al [17]. who worked on the evaluation of the wind potential using a hybrid Weibull approach because of the calm winds at the Lomé site. Since the approach used does not involve neural networks, we thought it appropriate to explore their approach given the notoriety of neural networks in non-linear regression.

The paper is organized as follows: Section 2 describes the classical methods used to evaluate wind potential and Section 3 describes the numerical methods used to evaluate wind potential. Section 4 discusses the statistical performance indicators used. In the fifth section, we present the calibrations made to obtain the ideal model for the simulation. Then, in section 6, we present our results and discussions resulting from the simulations at the two sites (Lomé and Cotonou) and conclude in section 7.

2 Classical method of wind distribution and numerical methods for wind potential assessment

The paper is organized as follows: Section 2 describes the classical methods used to evaluate wind potential and Section 3 describes the numerical methods used to evaluate wind potential. Section 4 discusses the statistical performance indicators used. In the fifth section, we present the calibrations made to obtain the ideal model for the simulation. Then, in section 6, we present our results and discussions resulting from the simulations at the two sites (Lomé and Cotonou) and conclude in section 7.

2.1 Estimation of Weibull parameters

The Weibull distribution is a widely used tool in statistical analysis [21]. In the context of wind energy, this tool will be used to understand the wind distribution at a production site and this is commonly referred to as the Weibull probability density function of wind speed. This function is characterized by three or two parameters [28], the most commonly used is the two-parameter function (1).

$$f(v) = \frac{k}{c}\left(\frac{v}{c}\right)^{k-1} \exp\left[-\left(\frac{v}{c}\right)^{k}\right] \tag{1}$$

where $f(v)$ is the distribution law or probability density , v is the wind speed expressed in (m/s), c is the scale factor, $k$is the shape factor characterizing the asymmetry of the distribution.
When k = 2 the distribution is called Rayleigh distribution which is a special case of the Weibull distribution. The cumulative function of the probability density function is given by (2) [3].

$$F(v) = 1 - \exp\left[-\left(\frac{v}{c}\right)^{k}\right] \tag{2}$$

In the literature several numerical methods are used to determine the parameters and the Weibull distribution: the Justus Empirical Method and the Maximum Likelihood Method, etc.

2.1.1 The Empirical Method of Justus (EMJ)

The form factor k and the scale factor c can be estimated by the following equation:

$$k = \left(\frac{\sigma}{\overline{v}}\right)^{-1,086} \tag{3}$$

$$c = \frac{\overline{v}}{\Gamma\left(1 + \frac{1}{k}\right)} \tag{4}$$

2.1.2 The Maximum Likelihood Method (MLM)

This is a very difficult method to solve and it is through numerical iterations that the parameters of the Weibull distribution are determined [29]. The parameters k and c are determined by equations (5) and (6).

$$k = \left[\left[\frac{\sum_{i=1}^{n} v_i^k \ln(v_i)}{\sum_{i=1}^{n} v_i^k}\right] - \left[\frac{\sum_{i=1}^{n} \ln(v_i)}{n}\right]\right]^{-1} \tag{5}$$

$$c = \left[\frac{\sum_{i=1}^{n} v_i^k}{n}\right]^{1/k} \tag{6}$$

2.2. The wind potential assessment

Wind potential is estimated by relationships (7) to (9).

- Energy available (E_a) at the site during a period T (30×24h for the month or 365 × 24h for the year) is given by (7). It is expressed in kWh/m².

$$E_a = \frac{T}{1000}.\frac{1}{2}\rho\int_0^{\infty} f(v).v^3 dv \tag{7}$$

Recoverable energy (E_r) at the site according to the characteristics of the wind turbine is given by the relation (8)

$$E_r = \frac{T}{1000}.\frac{1}{2}\rho S\left(\int_{V_s}^{V_r} f(v).v^3 dv + v_r^3\int_{V_r}^{V_c} f(v)dv\right) \text{ [kWh]} \tag{8}$$

- Energy produced (E_p) by the wind turbine is expressed by the relation (9)

$$E_p = \frac{T}{1000}\int_{V_s}^{V_c} f(v)P(v)dv \text{ [kWh]} \tag{9}$$

In relations (7) to (9):

- $f(v)$ is the wind speed distribution function;
- S is the area swept by the wind turbine blades;
- ρ is the air density, a parameter varying with latitude and temperature;
- v is the instantaneous wind speed;
- Vs is the starting speed of the wind turbine;
- Vr is the nominal speed of the wind turbine;
- Vc is the maximum speed of the wind turbine;
- $P(v)$ characterizes the power of the wind turbine as a function of the wind speed.

Wind turbine power curve modeling, which shows the relationship between wind speed and power, can be used as an important tool for monitoring and forecasting wind energy [30]. The wind turbine power curve is shown in Figure 1.

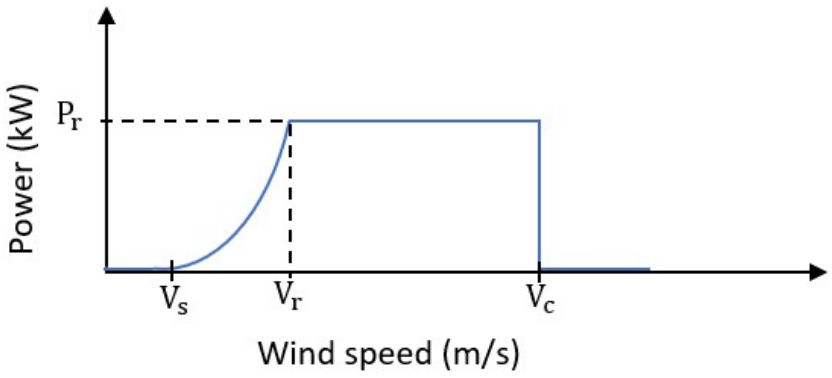

Figure 1. Power curve of a wind turbine.

The power curve characterizes how the wind turbine converts a range of speed into electric power. The power output $P(v)$ of the wind turbine as a function of the wind speed is given by (10).

$$P = \begin{cases} 0 & v < v_s \\ P_1(v) & v_s \le v \le v_r \\ P_r & v_r < v < v_c \\ 0 & v > v_c \end{cases} \tag{10}$$

This power is a simple expression except in the interval. In this interval $[v_s, v_r]$, the expression of the power can be approximated by (11).

$$P_1 = a_1 + b_1 v^k \tag{11}$$

where k is the Weibull constant already defined and a_1 and b_1 expressed by (12) and (13).

$$a_1 = \frac{P_r v_s^k}{v_s^k - v_r^k} \tag{12}$$

$$b_1 = \frac{P_r}{v_s^k - v_r^k} \tag{13}$$

3 Numerical methods for wind speed characterization

In this section we will examine two numerical approaches, the MLP approach and the SVR approach. The MLP approach is a neural network based method and the SVR approach is a maximum margin notion and kernel based method. They are widely used in pattern recognition, prediction, classification and regression analysis. They offer an alternative way to deal with complex and poorly defined problems [35].

3.1 MLP approaches

An Artificial Neuronal Network (ANN) is defined as a complex network made up of interconnected networks formed by elementary computer units (formal neurons). The neurons are organized in layers and can be connected in different ways. This topology of connection between neurons defines the architecture of the network and is related to the task to be performed. This task is often specified in the form of examples including a set of input values and a set of corresponding output values [3]. The network must "train" in order to be able to provide correct answers for other unknown inputs. Learning is a procedure for evaluating the network to meet performance criteria in order to minimize the error between the network output and the actual output value. Learning is performed according to an algorithm specific to the network architecture.
There are several types of ANNs. The MLP type ANNs are the most widely used, especially in nonlinear regression problems [31-32]. An MLP network consists of one or more hidden sigmoid layers as an activation function and an output layer. Figure 4 shows an example of a two-input MLP network comprising a three-neuron hidden layer and a neuron output layer. The neurons of the hidden layer L receive information from the neuron layer L-1 and are connected to the neuron layers L+1. There is no connection between neurons of the same layer. Each neuron of the output layer performs a non-linear function of the input layer. For more information on MLP, see [33-34]. The s_i potential of a neuron i and its activation O_i are given by relations (14) and (15), respectively

$$s_i = \sum_{j=1}^{p} w_{ij} x_j - b_j \tag{14}$$

$$O_i = h_i(s_i) \tag{15}$$

where *p* denotes the number of neurons of the upstream layer connected to the neurons xi; xj represents the input j of the network if the neuron i belongs to the first hidden layer, or, on the contrary, the neuron j represents the output *Oj* of the hidden layer which comes before the neuron *i*; w_{ij} is a constant scalar which represents the weight of the connection between the neuron i and the neuron j; bi is the bias; $h_i()$ the activation function of the neuron i. It can be different because it depends on whether the neuron is a hidden neuron or an output neuron. In general, hidden neurons have the same activation function which is the sigmoid function. Output neurons generally have the same activation function which is linear i.e. h(s)=s.

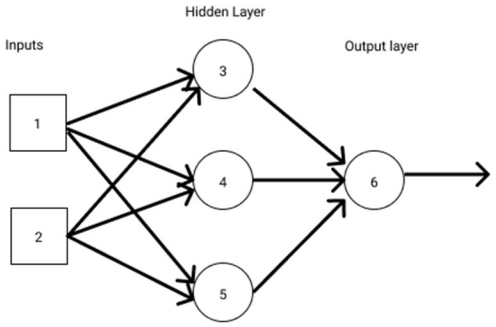

Figure 2. MLP structure.

3.2 SVR approaches

Derived from Support Vector Machine or Wide Margin Separators, (SVM) which are widely used tools in pattern recognition, prediction, classification and regression analysis [36-38]. SVMs achieve better performance compared to other traditional techniques such as neural networks and other conventional statistical models. The SVR can be divided into two categories depending on the problems faced. The linear SVR is available for linear problems and the non-linear SVR for more complex cases. The purpose of SVR is to approximate a set of data (x_i,y_i) by a function $f_{w,b}$.

$$f_{w,b}(x) = \langle w, x \rangle + b \tag{16}$$

in the linear case such as $\left| f_{w,b}(x_i) - y_i \right| \le \varepsilon$ with $i \in [1, n]$.

The idea is to minimize the term w while being under the constraint of not exceeding an error rate ε. From a graphical point of view, this is like finding an area of the plane that contains all the xi examples of width 2ε called tube. If we consider the minimization of we obtain the quadratic problem of the relation (17):

$$\begin{cases} \min\left\{\frac{1}{2}\|w\|^2\right\} \\ avec \begin{cases} y_i - \langle w, x_i \rangle - b \le \varepsilon \\ \langle w, x_i \rangle + b - y_i \le \varepsilon \end{cases} \end{cases} \tag{17}$$

This description of the problem therefore considers that a linear function that approximates all the examples with a precision exists. This is not always the case in practice. In the presence of outliers, it is also more important to allow some errors. In this case, the concept of flexible margin is used. It consists in introducing relaxation variables ξi, $\xi i*$ to
make the constraints of the optimization problem feasible, which becomes the relation (18);

$$\begin{cases} 0, for \left| y - f_{w,b}(x) \right| \le \varepsilon \\ \left| y - f_{w,b}(x) \right| - \varepsilon, for \left| y - f_{w,b}(x) \right| \succ \varepsilon \end{cases} \tag{18}$$

This function can be interpreted as creating a ray insensitivity tube ε around the $f_{w,b}(x)$. Going through the dual formulation and the Lagrange equation, the resulting function can be written as:

$$f(x)=\sum_{i=1}^{n}\left(\alpha_i+\alpha_i^*\right)\langle x_i,x\rangle+b \tag{19}$$

α_i and α_i^* are the Lagrange multipliers derived from the dual formulation.
As the data become more and more complex, nonlinear regression problems are solved with the use of kernel functions. That is, by projecting the data from the input space into a higher dimensional space. This is done in order to save time. The generalized form of the function becomes the relation (20).

$$f(x)=\sum_{i=1}^{n}\left(\alpha_i+\alpha_i^*\right)K(x_i,x)+b \tag{20}$$

The types of kernels available for solving nonlinear problems are listed in Table 1.

Table 1. Types of kernels.

Kernel	Function
Linear	$K(x,\mathrm{y})=\langle x,y\rangle$
Polynomial	$K(x,y)=\left(a\times\langle x,y\rangle+b\right)^d$
Gaussian	$K(x,y)=\exp\left(-\frac{\lVert x-y\rVert^2}{2\sigma^2}\right)$

4 Evaluating the performance of approaches

The performance of a calculation method is related to the margin of error that is obtained. The smaller the margin of error, the more efficient the method used.
In this work we used two performance indices, namely the square root means square error (RMSE) and the coefficient of determination (R^2).

$$RMSE=\sqrt{\frac{1}{n}\sum_{i=1}^{n}\left(X_{i,est}-X_{i,\mathrm{act}}\right)^2} \tag{21}$$

$X_{i,est}$ is the estimated value and $X_{i,act}$ is the observed value

$$R^2=\frac{\sum_{i=1}^{n}\left(X_{i,act}-X_{act,moy}\right)^2-\sum_{i=1}^{n}\left(X_{i,est}-X_{i,act}\right)^2}{\sum_{i=1}^{n}\left(X_{i,act}-X_{act,moy}\right)^2} \tag{22}$$

$X_{act,moy}$ is the mean value of the measured or observed data and X_{est} is the estimated value.

5 Calibration

In this section, we determine the best settings for the Cotonou and Lomé sites with the different approaches discussed.

5.1 Weibull parameters from distribution-based methods

The values of the Weibull k and c parameters are calculated according to the different classical methods used (EMJ and MLM) and the results are presented in Table 2. Using the factors found the modelling of the Weibull distribution will be done.

Table 2. Weibull parameters obtained from EMJ and MLM for the sites of Cotonou and Lomé.

Methods	Lomé		Cotonou	
	k	c	k	c
EMJ	1,8233	3,9704	2,3671	4,5264
MLM	2,0310	4,1788	2,5722	4,6173

5.2 MLP

In order to be able to adjust the histogram of wind speed frequencies, we have defined a MLP with two (02) inputs, which will be dedicated to wind speeds and frequencies, and only one output, which will be the speed frequencies. For the hidden layer the number of neurons of the hidden layer after several tests is set to 9 and we have chosen a single neuron for the output. The result of the tests is obtained by varying the number of neurons in the hidden layer from 4 to 10.

Table 3. Choice of the number of neurons.

Nombre de Neurones	RMSE	
	Lomé	Cotonou
4	0,00184301	0,00534417
5	0,00167651	0,00488000
6	0,00038814	0,00487000
7	0,00041508	0,00126947
8	0,00041634	0,00001450
9	0,00008020	0,00001380
10	0.0009560	0,00001980

5.3 SVR

To determine the fit of the wind speed frequency histogram, wind speeds are used as input to the SVR model and speed frequencies are used as output. Since the problem we are working on is non-linear, we used kernel functions to find the best function. The RMSE is used here to make the comparison to find the best result. Table 4 shows the results of the tests for the different locations. According to the results, the Gaussian kernel is the one with the best performance.

Table 4. Comparison of SVR kernels.

Kernels	RMSE	
	Lomé	Cotonou
Linear	0.056404569	0,133998139
Polynomial	0,041952826	0,084815911
Gauss	0,000704443	0,003901821

6 Results and discussion

The purpose of this article is to carry out a comparative evaluation of wind potential assessment methods in Togo and Benin, the case study includes the following four steps:

- For each of the four methods EMJ, MLM, MLP and SVR, we obtain the probability density function of the wind speed or distribution law $f_j(v)$ by using as input the measured wind speed series
- We fit the obtained probability densities to the frequency histograms and derive the approximation errors of the distribution e_j
- Then we calculate the energy potentials E_j using the power curve of the wind turbines and evaluate the associated energy errors ξ_j
- Finally, the methods for evaluating energy potential are compared on the basis of performance indicators, which are the RMSE and the R^2

6.1 Wind speed characterization performance

To verify that the results obtained by the three approaches are distributional laws, the integral given by the relation must be calculated (23). If this integral is equal to 1 then these results obtained will be considered as laws of distribution. Table 5 shows the results of the calculation.

Table 5. Distribution area.

	MLP	SVR
Lomé	0.996	0.995
Cotonou	0.997	0.996

The results in the table tend towards 1, so we can say that they are distribution laws.

$$\int_0^{v_{max}} f(v).dv = 1 \tag{23}$$

Figures 3 and 4 show the distribution function curves for fitting the annual wind frequency histograms for the two sites. Performance evaluation metrics described in previous section are presented in Table 6 to compare the performance of the five methods. Results show a better performance of the MLP approaches compared to the other approaches used, regardless of the wind site. These results compared to the work of Asghar and al. show that the MLP approach fitted the distribution curve better than the neuro-fuzzy approach [21] (0.00005016 versus 0.0014294 for the RMSE). We also observe the performance of this approach compared to the work of Salami et al [17]. based on the consideration of calm winds at the Lomé site. The MLP approach fits the distribution better than the Hybrid Weibull approach used (0.95%).

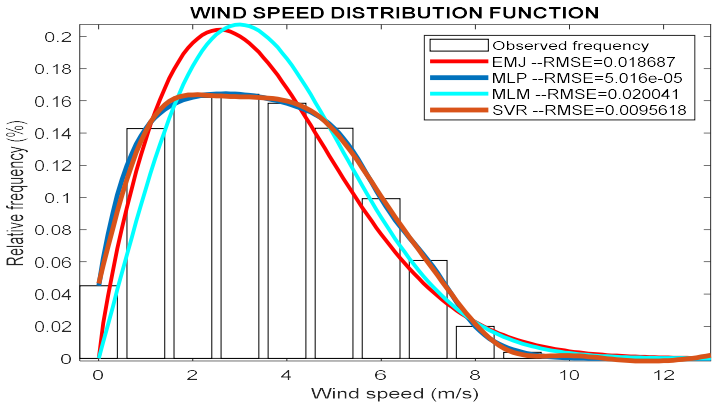

Figure 3. Wind speed distribution function for the site of Lomé.

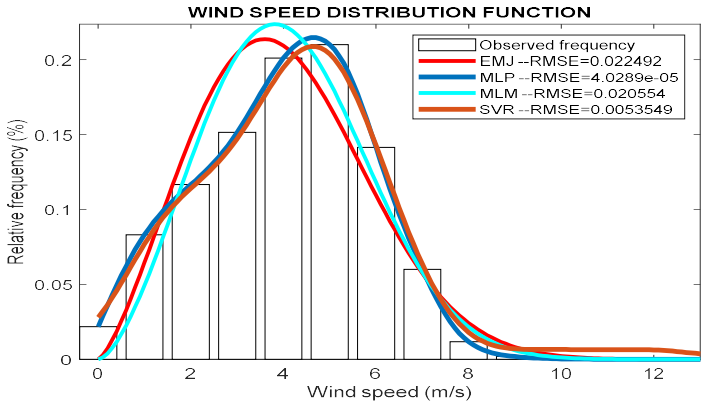

Figure 4. Wind speed distribution function for the site of Cotonou.

In order to compare the approaches used, the performance indicators for each approach are listed in Table 6. The results show that the MLP approach prevails over the others regardless of the site.

6.2 Wind turbine

In our work, we based our choice of the E-48 wind turbine in ENERCON reviews [39]. Its characteristics are given in Table 7.

Table 6. Characteristics of E-48.

Name	E-48
Cut-in speed (m/s)	3
Rated speed (m/s)	12
Cut-out speed (m/s)	25
Rated output power (kW)	800
Blade diameter (m)	48
Hub(m)	76

Normally the cut-off speed will vary between 28 and 34 ms-1. However, in our study, a speed of 25 ms^{-1} was assumed due to the absence of the power curve beyond this speed.
Figure 5 shows the wind power curve of E-48 as modeled by the constructor as well as using the numerical methods discussed in this paper.

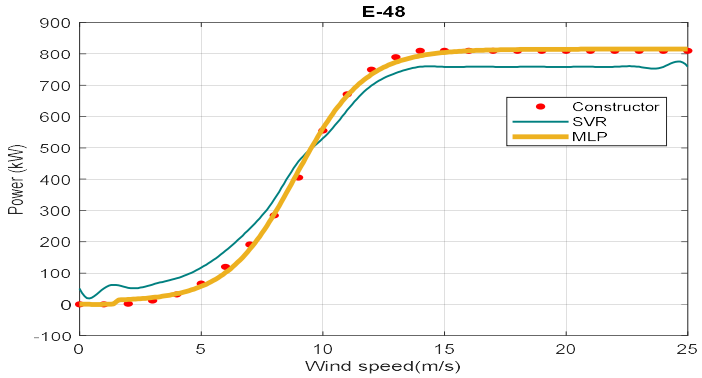

Figure 5. Characteristic power curve modeling for E-48.

Table 7. Method comparison.

	EMJ		MLP		MLM		SVR	
	R^2	RMSE	R^2	RMSE	R^2	RMSE	R^2	RMSE
Lomé	0.9687	0.0187	1.000	0.000	0.9649	0.020	0.9841	0.009
Cotonou	0.9570	0.0220	1.000	0.000	0.9670	0.021	0.9989	0.005

Since wind speed measurements have not been taken at the altitude where the turbines will be deployed, it is necessary to extrapolate the wind speed values at the hub height of the turbine using the vertical wind profile power law model proposed by Hellman [40] and expressed in equation (24).

$$\frac{v}{v_0} = \left(\frac{h}{h_0} \right)^{\alpha} \tag{24}$$

Where v is the wind speed at altitude h and v_0 the speed at reference altitude h_0. The wind shear coefficient or coefficient of friction α, generally ranges from 0.40 in areas with tall buildings to 0.10 on smooth, hard ground, lakes or the ocean. For Lomé and Cotonou, as the measurements were taken in airport areas, we chose α=0.1 in this study.

6.3 Wind potential estimation

In this section, we compare the accuracy of the energy potential estimates of the four methods (EMJ, MLM, MLP, and SVR). The comparison is made with the observed energy potential which is obtained by calculating the energy potential using the time series of the measured raw wind speed and the wind power curve of the selected turbine manufacturer. Three quantities of energy are taken into account for the comparison: the available energy per unit area Ea in kWh/m^2, the recoverable energy Er in kWh and the produced energy Ep in kWh.

6.3.1 Available energy

Table 8 presents the energy available per unit area observed monthly and estimated by the methods. To show the comparison between the results of the approaches used, we present the correlations between the observed and estimated available energy on figures 6 and 7. The RMSE of the MLP approach is at least three orders of magnitude lower than that of the other three methods. The RMSE tends to overestimate the energy density at the Lomé site.

6.3.2 Recoverable energy

As previously, a comparison was made between the monthly recoverable energy Er in kWh respectively at the Lomé and Cotonou sites and the observed or actual recoverable energy values which are calculated from the measured wind speed data (see Table 9). Figures 8 and 9 show the correlation between observed and estimated recoverable energy for the Lomé and Cotonou sites respectively.
The correlation graphs in Figures 10 and 11 show that the MLM and EMJ lead to the most inaccurate estimates of recoverable energy. In fact, for both sites, these methods underestimate the recoverable energy values. This behaviour results from the Weibull distribution methods overestimating the density of low velocities. Although the SVR gives acceptable estimates for the Lomé site, its RMSE at the Cotonou site is of the same order of magnitude as those of MLM and EMJ. As with the estimates of available energy, MLP ranks first with more accurate estimates.

6.3.3 Produced energy

Table 10 shows the energy produced or wind power generation Ep in kWh at the Lomé and Cotonou sites. The observed or actual energy production calculated from the measured wind speed data is compared to the estimated wind energy production. Figures 14 and 15 show the correlation between observed and estimated energy production for the Lomé and Cotonou sites respectively.

The results of the correlation study show that MLM and EMJ methods based on the Weibull distribution systematically underestimate the energy output of wind turbines. Although the SVR obtains acceptable estimates at the Lomé site, it mainly underestimates wind energy production values at the Cotonou site. The MLP proves to be the most accurate for both sites, as shown in Figures 12 and 13.

Table 8. Available energy density estimation (kWh/m^2).

	Lomé					Cotonou				
Month	Obs.	MLP	SVR	EMJ	MLM	Obs.	MLP	SVR	EMJ	MLM
Jan.	43,62	43,29	52,60	44,50	46,59	46,10	46,14	59,59	45,42	46,16
Feb.	77,54	77,71	92,71	80,45	82,72	87,52	87,08	79,94	91,47	90,32
Mar.	87,74	88,10	121,17	90,42	92,63	96,84	96,84	89,27	101,89	100,09
Apr.	69,97	70,31	171,06	72,89	75,42	82,69	82,80	78,76	85,44	85,56
May	46,96	48,73	43,74	48,30	50,29	57,68	58,35	70,34	58,15	59,47
June	57,86	57,34	66,50	59,75	61,82	71,41	71,33	89,29	74,04	75,48
July	89,85	89,35	114,59	91,98	92,42	116,59	116,62	133,49	120,70	119,51
Aug.	110,61	111,26	158,28	112,40	112,03	118,36	117,46	143,79	122,18	121,85
Sep.	92,35	92,95	110,75	94,20	94,97	100,96	100,83	116,15	106,59	105,99
Oct.	57,34	57,33	64,77	58,94	60,81	58,21	58,01	66,62	59,62	60,64
Nov.	44,90	44,88	56,86	45,91	47,50	52,70	52,80	66,44	52,41	52,70
Dec.	39,55	39,62	52,62	40,12	41,83	47,09	47,10	61,45	46,21	46,62

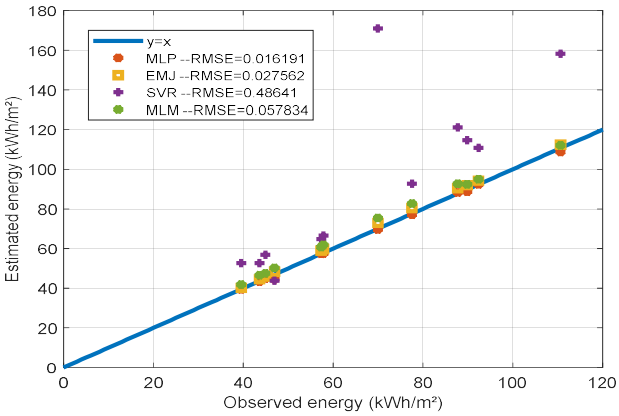

Figure 6. Correlation between observed and estimated available energy density for Lomé.

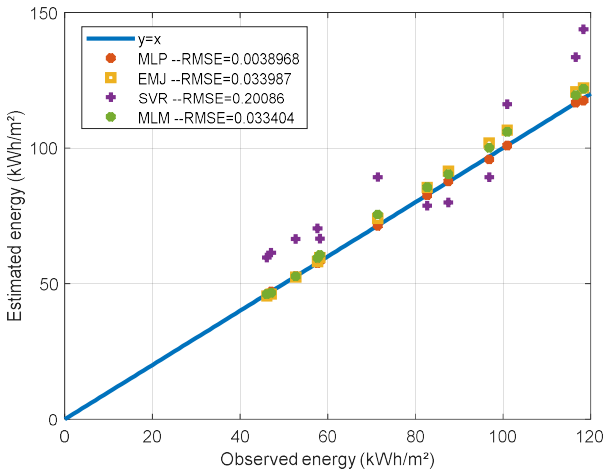

Figure 7. Correlation between observed and estimated available energy density for Cotonou.

Table 9. Recoverable energy estimation (kWh).

	Lomé					Cotonou				
Month	Obs.	MLP	SVR	EMJ	MLM	Obs.	MLP	SVR	EMJ	MLM
Jan.	1338,96	1487,41	1543,50	576,84	911,75	1575,35	1632,74	1741,70	675,97	821,84
Feb.	2256,12	2400,51	2397,26	982,80	1263,56	3028,02	3135,22	2259,32	1322,18	1484,56
Mar.	2728,72	2689,27	2761,58	1084,95	1373,65	3628,73	3466,82	2322,58	1484,77	1679,00
Apr.	2555,64	2271,76	2391,24	892,63	1186,90	3149,38	2886,74	2281,55	1199,76	1415,63
May	1962,82	1673,98	1642,78	607,58	905,78	2288,98	1972,34	1861,55	809,24	1007,27
June	2026,72	2045,79	2033,82	749,78	1006,57	2508,27	2490,53	2392,91	987,93	1272,66
July	2933,38	3059,06	3135,84	1225,42	1365,74	3736,94	3904,56	3350,62	1701,40	1823,20
Aug.	3496,85	3610,83	3655,80	1532,22	1606,99	4325,46	4133,44	3930,85	1836,23	1926,84
Sep.	3257,28	3101,21	3118,39	1206,89	1345,47	3849,82	3590,79	3449,54	1457,29	1782,36
Oct.	2403,33	2087,76	2022,03	745,97	967,02	2531,42	2052,42	1894,93	838,57	1028,53
Nov.	2001,16	1812,64	1920,72	615,12	831,77	2119,30	1919,72	1764,69	795,16	919,93
Dec.	1718,32	1614,71	1728,40	537,15	806,48	1857,41	1732,89	1833,68	701,57	813,13

Table 10. Wind turbine output energy estimation (kWh).

	Lomé					Cotonou				
Month	Obs.	MLP	SVR	EMJ	MLM	Obs.	MLP	SVR	EMJ	MLM
Jan.	44819,60	44805,30	54004,19	40591,66	45473,75	47268,98	47317,13	61302,58	45494,08	46781,36
Feb.	80666,95	80371,97	89951,98	79225,91	83570,95	92295,19	92479,42	80897,66	95352,61	94657,03
Mar.	91143,12	91333,28	115021,50	88836,31	93463,65	102517,44	101898,57	90686,23	106856,16	105490,33
Apr.	72372,36	72281,81	112155,15	71901,73	76209,15	86458,74	86376,54	78097,55	88347,20	89214,99
May	48072,94	47625,44	42527,44	47417,46	50712,13	58957,99	58815,27	60432,51	59142,45	61048,44
June	59907,14	59463,21	63890,18	58877,55	62420,96	74447,50	74353,51	85634,60	74949,03	77799,98
July	94292,97	93343,02	114702,58	94203,07	95524,21	122945,80	123028,00	135774,10	126909,05	126143,37
Aug.	115991,63	114254,39	152781,04	116972,61	116997,09	125951,93	124789,52	152155,07	130072,52	129943,30
Sep.	98024,08	98078,04	116612,05	93053,45	95641,97	108463,80	107869,25	124577,80	105378,70	109467,25
Oct.	60993,18	61047,57	67561,40	57185,18	61151,65	60397,15	60154,68	60736,78	60828,04	62378,37
Nov.	50490,76	50490,78	62900,26	47248,99	50637,15	54363,16	54502,78	58051,67	53762,00	54173,96
Dec.	44669,80	44758,06	58326,92	41867,41	45427,11	48226,40	48168,58	57147,80	47100,35	47592,87

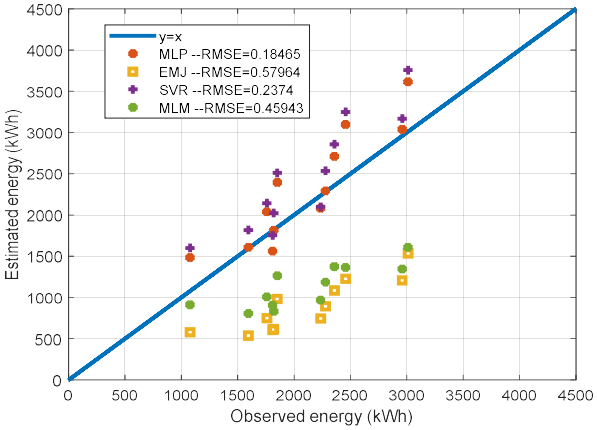

Figure 8. Correlation between observed and estimated recoverable energy on the site of Lomé.

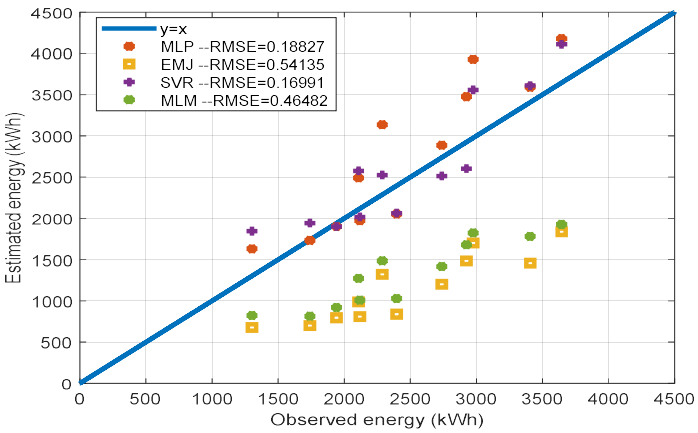

Figure 9. Correlation between observed and estimated recoverable energy on the site of Cotonou.

7 Conclusion

This study of wind energy resource assessment in Benin and Togo, two West African countries, examines four methods for assessing wind energy potential: MLP, SVR, EMJ, and MLM.As expected, the results of the case studies confirm that accurate estimation of the wind speed distribution law has a significant impact on wind potential assessment. The comparison of the performances of the methods studied in this work shows that the MLP approach, with an RMSE of 0.00005016 for the Lomé site and 0.000040289 for the Cotonou site, is the best method for evaluating the wind potential at the Togo and Benin sites. The SVR method is in second place with an RMSE of 0.0095618 for the Lomé site and 0.0053549 for the Cotonou site.

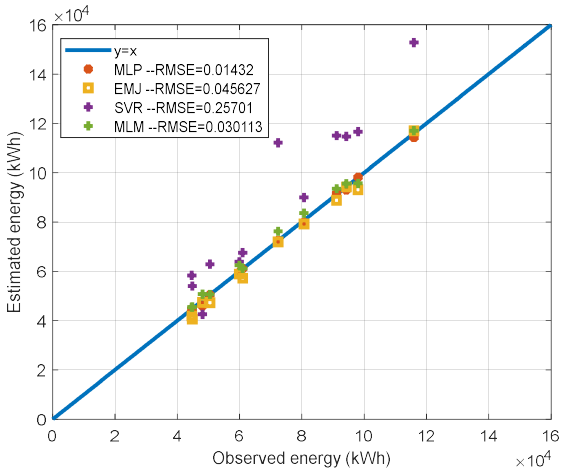

Figure 10. Correlation between observed and estimated wind energy output on the site of Lomé.

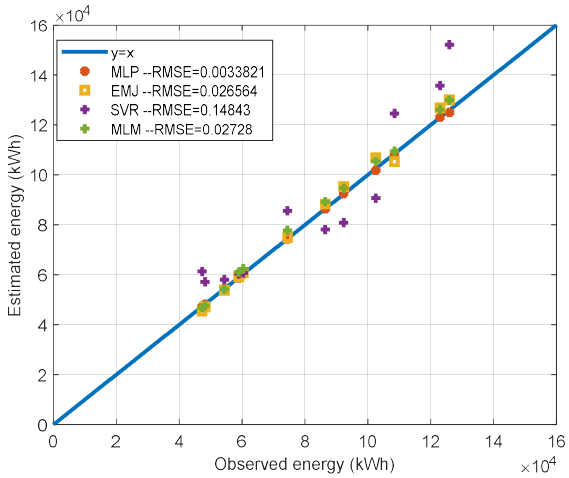

Figure 11. Correlation between observed and estimated wind energy output on the site of Cotonou.

These two methods based respectively on neural networks and regression are clearly more efficient than the other two methods studied in this work, for the estimation of the energy produced per unit area, the recoverable energy and the wind energy production for the two wind sites. Although the Weibull distribution is widely used in the assessment of wind energy potential for wind farm sites, this study showed that the two methods based on the Weibull distribution, EMJ and MLM, lead to the least accurate estimates, particularly in the quantification of recoverable energy and wind turbine production. Although ~~the~~ SVR is the second most important method used for The study, it is unstable depending on the type of estimate and the wind site. Its performance is not uniform for the two sites and it is less recommended for the Cotonou site. Therefore, the best method for estimating wind potential recommended for the Lomé (Togo) and Cotonou (Benin) sites is the MLP based on the neural system with 9 neurons in the hidden layer. To summarize, the SVR and MLP approaches, once calibrations are well done, are good leads in wind potential assessment for any site. In sum,

the different approaches used have made it possible to evaluate the wind energy potential on the two sites. On average, the energy available annually on the Lomé site is evaluated at 68.40 kWh/m² by the MLP, 92.13 kWh/m² by the SVR against 68.19 kWh/m² for the real value. For the Cotonou site the average is around 77.95 kWh/m² for the MLP, 87.93 kWh/m² for the SVR against 78.01 for the observed average.
The annual recoverable averages are estimated respectively as follows 2389.94 kWh for the observed,2321.24 for the MLP and 2362.61 for the SVR on the site of Lomé and that of Cotonou: 2883.26 kWh, 2743.18kW and 2423.66 kWh respectively for the observed value, MLP and SVR approaches. With the E-48 aerogenerator, installed at an altitude of 76m, the average energy produced during the year is 71787.04 kWh at the Lomé site and the estimates by the different approaches give 71487.74 kWh for the MLP and 87536.22 for the SVR. At the Cotonou site we observe 81857.84 kWh against 81644.10 kWh for the MLP and 87124.53 for the SVR.

References

[1] Emeksiz, C., & Demirci, B. (2019). The determination of offshore wind energy potential of Turkey by using novelty hybrid site selection method. *Sustainable Energy Technologies and Assessments*, *36*, 100562.

[2] Afonso, T. L., Marques, A. C., & Fuinhas, J. A. (2017). Strategies to make renewable energy sources compatible with economic growth. *Energy strategy reviews*, *18*, 121-126.

[3] Thiaw, L., Sow, G., Fall, S. S., Kasse, M., Sylla, E., & Thioye, S. (2010). A neural network based approach for wind resource and wind generators production assessment. *Applied Energy*, *87*(5), 1744-1748.

[4] Li, G., & Shi, J. (2010). Application of Bayesian model averaging in modeling long-term wind speed distributions. *Renewable Energy*, *35*(6), 1192-1202.

[5] Morgan, E. C., Lackner, M., Vogel, R. M., & Baise, L. G. (2011). Probability distributions for offshore wind speeds. *Energy Conversion and Management*, *52*(1), 15-26.

[6] Carta, J. A., Ramírez, P., & Velázquez, S. (2008). Influence of the level of fit of a density probability function to wind-speed data on the WECS mean power output estimation. *Energy Conversion and Management*, *49*(10), 2647-2655.

[7] Masseran, N., Razali, A. M., Ibrahim, K., Zaharim, A., & Sopian, K. (2013). The probability distribution model of wind speed over East Malaysia. *Research Journal of Applied Sciences, Engineering and Technology*, *6*(10), 1774-1779.

[8] Saleh, H., Aly, A. A. E. A., & Abdel-Hady, S. (2012). Assessment of different methods used to estimate Weibull distribution parameters for wind speed in Zafarana wind farm, Suez Gulf, Egypt. *Energy*, *44*(1), 710-719.

[9] Celik, A. N. (2003). Weibull representative compressed wind speed data for energy and performance calculations of wind energy systems. *Energy Conversion and Management*, *44*(19), 3057-3072.

[10] Murthy, K. S. R., & Rahi, O. P. (2019). Wind power density estimation using rayleigh probability distribution function. In *Applications of Artificial Intelligence Techniques in Engineering* (pp. 265-275). Springer, Singapore.

[11] Ahmed, A. S. (2018). Wind energy characteristics and wind park installation in Shark El-Ouinat, Egypt. *Renewable and Sustainable Energy Reviews*, *82*, 734-742.

[12] Azad, A. K., Rasul, M. G., Alam, M. M., Uddin, S. A., & Mondal, S. K. (2014). Analysis of wind energy conversion system using Weibull distribution. *Procedia Engineering*, *90*, 725-732.

[13] Elamouri, M., & Amar, F. B. (2008). Wind energy potential in Tunisia. *Renewable energy*, *33*(4), 758-768.

[14] Kiss, P., & Jánosi, I. M. (2008). Comprehensive empirical analysis of ERA-40 surface wind speed distribution over Europe. *Energy Conversion and Management*, *49*(8), 2142-2151.

[15] Celik, A. N. (2004). A statistical analysis of wind power density based on the Weibull and Rayleigh models at the southern region of Turkey. *Renewable energy*, *29*(4), 593-604.

[16] Safari, B., & Gasore, J. (2010). A statistical investigation of wind characteristics and wind energy potential based on the Weibull and Rayleigh models in Rwanda. *Renewable Energy*, *35*(12), 2874-2880.

[17] Salami, A. A., Ajavon, A. S. A., Kodjo, M. K., & Bedja, K. S. (2013). Contribution to improving the modeling of wind and evaluation of the wind potential of the site of Lome: Problems of taking into account the frequency of calm winds. *Renewable Energy*, *50*, 449-455.

[18] Rocha, P. A. C., de Sousa, R. C., de Andrade, C. F., & da Silva, M. E. V. (2012). Comparison of seven numerical methods for determining Weibull parameters for wind energy generation in the northeast region of Brazil. *Applied Energy*, *89*(1), 395-400.

[19] Justus, C. G., Hargraves, W. R., Mikhail, A., & Graber, D. (1978). Methods for estimating wind speed frequency distributions. *Journal of applied meteorology, 17(3), 350-353.*

[20] Weisser, D. (2003). A wind energy analysis of Grenada: an estimation using the 'Weibull'density function. *Renewable energy*, *28*(11), 1803-1812.

[21] Asghar, A. B., & Liu, X. (2018). Estimation of wind speed probability distribution and wind energy potential using adaptive neuro-fuzzy methodology. *Neurocomputing*, *287*, 58-67.

[22] Tizgui, I., El Guezar, F., Bouzahir, H., & Benaid, B. (2017). Comparison of methods in estimating Weibull parameters for wind energy applications. *International Journal of Energy Sector Management*, *11*(4), 650-663.

[23] Mabel, M. C., & Fernandez, E. (2009). Estimation of energy yield from wind farms using artificial neural networks. *IEEE Transactions on energy conversion*, *24*(2), 459-464.

[24] A.N. CELIK, M. KOLHE, Generalized feed-forward based method for wind energy prediction, *Appl. Energy 101 (2013) 582-588.*

[25] T.P. Chang, Performance comparison of six numerical methods in estimating Weibull parameters for wind energy application, *Appl. Energy 88 (2011) 272-282.*

[26] Seguro, J. V., & Lambert, T. W. (2000). Modern estimation of the parameters of the Weibull wind speed distribution for wind energy analysis. *Journal of wind engineering and industrial aerodynamics*, *85*(1), 75-84.

[27] Singh, S., Bhatti, T. S., & Kothari, D. P. (2007). Wind power estimation using artificial neural network. *Journal of Energy Engineering*, *133*(1), 46-52.

[28] Wais, P. (2017). Two and three-parameter Weibull distribution in available wind power analysis. *Renewable energy*, *103*, 15-29.

[29] Kidmo, D. K., Danwe, R., Doka, S. Y., & Djongyang, N. (2015). Statistical analysis of wind speed distribution based on sixWeibull Methods for wind power evaluation in Garoua, Cameroon. *Journal of Renewable Energies*, *18*(1), 105-125.

[30] Seo, S., Oh, S. D., & Kwak, H. Y. (2019). Wind turbine power curve modeling using maximum likelihood estimation method. *Renewable energy*, *136*, 1164-1169.

[31] Hornik, K., Stinchcombe, M., & White, H. (1989). Multilayer feedforward networks are universal approximators. *Neural networks*, *2*(5), 359-366.

[32] Dotche, K. A., Salami, A. A., Kodjo, K. M., Sekyere, F., & Bedja, K. S. (2019, August). Artificial Neural Network Approach for the Integration of Renewable Energy in Telecommunication Systems. In *2019 IEEE PES/IAS PowerAfrica* (pp. 279-284). IEEE.

[33] Li, S., O'Hair, E., & Giesselmann, M. G. (1997). Using neural networks to predict wind power generation. In *Proceedings of the 1997 International Solar Energy Conference*.

[34] Li, S., Wunsch, D. C., O'Hair, E., & Giesselmann, M. G. (2001). Comparative analysis of regression and artificial neural network models for wind turbine power curve estimation. *J. Sol. Energy Eng.*, *123*(4), 327-332.

[35] Kalogirou, S. A. (2000). Applications of artificial neural-networks for energy systems. *Applied energy*, *67*(1-2), 17-35.

[36] Asefa, T., Kemblowski, M., McKee, M., & Khalil, A. (2006). Multi-time scale stream flow predictions: The support vector machines approach. *Journal of hydrology*, *318*(1-4), 7-16.

[37] Dotche, K. A., Salami, A. A., Kodjo, K. M., Ouro-Agbake, H., & Bedja, K. S. (2019, August). Wind Speed Prediction Based on Support Vector Regression Method: a Case Study of Lome-Site. In *2019 IEEE PES/IAS PowerAfrica* (pp. 267-272). IEEE.
2019 IEEE PES/IAS PowerAfrica, Abuja, Nigeria, 2019, pp. 267-272.

[38] Wang, Y., & Liu, X. (2015). Improved support vector clustering algorithm for color image segmentation. Engineering Review: *Međunarodni časopis namijenjen publiciranju originalnih istraživanja s aspekta analize konstrukcija, materijala i novih tehnologija u području strojarstva,*

brodogradnje, temeljnih tehničkih znanosti, elektrotehnike, računarstva i građevinarstva, 35(2), 121-129.

[39] ENERCON. E-48. [Online]. Available: https://www.enercon.de/fr/produits/ep-1/e-48/, 2020.

[40] Hellmann, G. (1914). Über die Bewegung der Luft in den untersten Schichten der Atmosphäre: Kgl. *Akademie der Wissenschaften [G.] Reimer*.